Inorganic Chemistry

pubs.acs.org/IC

Article

Direct Evidence for an Intermediate Multiferroic Phase in $LiCuFe_2(VO_4)_3$

Xiyu Chen,[#] Shuhan Zheng,[#] Meifeng Liu,[*] Tao Zou, Wei Wang, Keer Nie, Fei Liu, Yunlong Xie, Min Zeng, Xiuzhang Wang, Hong Li, Shuai Dong,[*] and Jun-Ming Liu

Cite This: *Inorg. Chem.* 2022, 61, 944−949

Read Online

ACCESS | Metrics & More | Article Recommendations

ABSTRACT: Magnetic susceptibility, specific heat, dielectric, and electric polarization of $LiCuFe_2(VO_4)_3$ have been investigated. Two sequential antiferromagnetic transitions at $T_{N1} \sim 9.95$ K and $T_{N2} \sim 8.17$ K are observed under zero magnetic field. Although a dielectric peak at T_{N1} is clearly identified, the measured pyroelectric current also exhibits a sharp peak at T_{N1}, implying the magnetically relevant ferroelectricity. Interestingly, another pyroelectric peak around T_{N2} with an opposite signal is observed, resulting in the disappearance of electric polarization below T_{N2}. Besides, the electric polarization is significantly suppressed in response to external magnetic field, evidencing a remarkable magnetoelectric effect. These results suggest the essential relevance of the magnetic structure with the ferroelectricity in $LiCuFe_2(VO_4)_3$, deserving further investigation of the underlying mechanism.

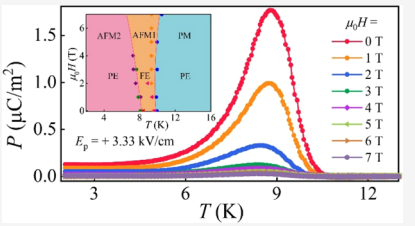

INTRODUCTION

The exploration and synthesis of novel multiferroics have been one of the major interests in condensed matter physics. In multiferroics, magnetism and ferroelectricity coexist, which allows the control of magnetization M by electric field E or electrical polarization P by magnetic field H.[1−7] Therefore, multiferroics have huge potential applications in novel electronic devices, such as memories, sensors, and so forth.[4,8] Depending on the origin of ferroelectricity, multiferroics are distinguished into two types.[1,9] In type-I multiferroics, the magnetism and ferroelectricity have distinctly different origins and the magnetoelectric (ME) coupling is usually weak. For type-II multiferroics, polarization P is generated by specific magnetic structures, leading to a strong ME effect. Now, it is well known that the ferroelectricity in type-II multiferroics originates from spin−orbit coupling or spin−lattice coupling.[1,3] For instance, the ferroelectricity in $TbMnO_3$ and $Ba_2XGe_2O_7$ (X = Mn, Co, and Cu) is induced by inverse Dzyaloshinskii−Moriya interaction and spin-dependent p-d hybridization, respectively.[10−12] These materials have noncollinear spin orders, and the spin−orbit coupling dominates. Besides, in materials such as Ca_3CoMnO_6, the P is induced by the exchange striction effect in collinear up-up-down-down spin order, which is dominated by spin−lattice coupling.[13,14] It is noted that these couplings belong to a high-order quantum effect and the induced P is usually small. Even worse, the magnetic ordering temperature in type-II multiferroics is usually low. Therefore, currently available multiferroics are not suitable for application yet. Continuous efforts have been paid to explore novel materials, such as $CaMn_7O_{12}$, $BiMn_3Cr_4O_{12}$, and so forth.[15−18] However, the difficulties remain, and searching for new multiferroics is still a major issue in this area.

Frustrated quasi-one-dimensional (quasi-1D) antiferromagnets have received widespread interest due to the rich and largely unexplored physics, such as quantum criticality,[19,20] H-induced magnetic ordering,[21] quantum spin liquid,[22] and so forth. Owing to the highly frustrated magnetic interactions, multiferroicity induced by non-collinear spin order is expected in quasi-1D magnetic systems. In fact, this issue has been explored in quasi-1D systems such as Cu-base quantum spin-chain $LiCu_2O_2$[23] and $LiCuVO_4$,[24] pyroxene $NaFeGe_2O_6$[25] and $SrMnGe_2O_6$,[26] and zigzag-chain $MnWO_4$.[27] In these materials, a strong ME effect, such as H switching P, has been extensively investigated. Considering the large number of quasi-1D materials, it is valuable to explore further the quasi-1D magnetic systems, addressing the multiferroicity.

From this perspective, a recently reported quasi-1D mixed spin-chain triple vanadate $LiCuFe_2(VO_4)_3$ attracted research interests in the multiferroic community. $LiCuFe_2(VO_4)_3$ was first synthesized by Belik,[28] and its crystal structure is shown in Figure 1a,b. Neighboring FeO_6 octahedra and CuO_5 triangular bipyramids are connected by edge sharing and form quasi-1D Cu^{2+}-Fe^{3+} mixed spin chains. According to earlier work, the frustration factor $f = |\theta_{CW}|/T_N$ for $LiCuFe_2(VO_4)_3$ is 12, where

Received: September 24, 2021
Published: December 29, 2021

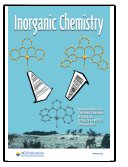

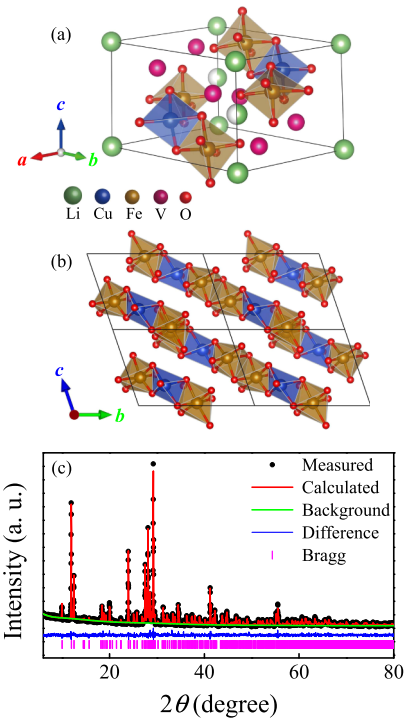

Figure 1. (a,b) Schematic of the crystal structure of $LiCuFe_2(VO_4)_3$. The unit cells are indicated by black boxes. (c) Rietveld refined powder X-ray spectrum of $LiCuFe_2(VO_4)_3$ at room temperature.

θ_{CW} is the Curie–Weiss constant and T_N is the magnetic ordering temperature,[29] suggesting a highly frustrated spin structure in $LiCuFe_2(VO_4)_3$. Besides, the first-principles calculation indicated the competition of ferromagnetic and antiferromagnetic (AFM) exchanges, which may lead to a non-collinear spin order and induce ferroelectricity.[30] Very recently, indirect evidences in terms of ferroelectricity and ME effects in $LiCuFe_2(VO_4)_3$ were reported,[30,31] while direct measurement of polarization P is absent.

In this work, we present a comprehensive study of $LiCuFe_2(VO_4)_3$ including the magnetic susceptibility, specific heat, and electric polarization measurements. It will be revealed that $LiCuFe_2(VO_4)_3$ undergoes two successive AFM transitions at $T_{N1} \sim 9.95$ K and $T_{N2} \sim 8.17$ K, as evidenced by magnetic susceptibility and specific heat. Very interestingly, two sign-opposite pyroelectric peaks at T_{N1} and T_{N2}, marking the generation and disappearing of polarization P, respectively, are identified. The ME effect in terms of variable polarization P under different H is also presented.

EXPERIMENT

Polycrystalline samples of $LiCuFe_2(VO_4)_3$ were synthesized by the conventional solid–state reaction method. The stoichiometric mixtures of Li_2CO_3, CuO, Fe_2O_3, and V_2O_5 were sufficiently ground and fired at 600 °C for 24 h in air. The obtained powders were reground and pelleted. Then, the resulting pellets were sintered at 640 °C for 72 h in air again with three intermediate regrinding and pelleting processes. Eventually, the phase purity of powder samples was analyzed using an X-ray diffractometer (SmartLab SE, Rigaku) with Cu Kα radiation at room temperature (T).

The dc magnetic susceptibility $\chi(T)$ as a function of T under different magnetic fields H was measured using a physical property measurement system (PPMS DynaCool-9, Quantum Design). The specific heat (C_p) was also measured using PPMS DynaCool-9 based on the heat relaxation method.

For electrical measurement, Au electrodes were deposited on the top and bottom sides of the disk-like sample (3.25 mm in diameter and 0.3 mm in thickness). The measurements were carried out in a PPMS, which provides magnetic field and a cryogenic environment. The dielectric constant ε_r was measured using an LCR meter (Agilent E4980A). For pyroelectric current (I_{pyro}) measurement, the poling electric field E_p was provided using a Keithley 6517B electrometer. Before the measurement, the sample was cooled from 15 to 2 K under $E_p = \pm 3.33$ kV/cm. When the sample temperature was cooled to 2 K, the poling electric field was removed and the sample was short-circuited for 30 min to remove the trapped charge. Then, the pyroelectric current was recorded using the Keithley 6517B electrometer when raising the temperature. The P is derived by integrating the pyroelectric current. It is noted that the magnetic field remained unchanged during the pyroelectric measurement.

RESULTS

Figure 1c displays the measured X-ray spectrum of $LiCuFe_2(VO_4)_3$ powders. No stray peaks are identified, suggesting the high purity of $LiCuFe_2(VO_4)_3$. The diffraction patterns are further analyzed by Rietveld refinement.[32,33] The space group of $LiCuFe_2(VO_4)_3$ is fitted to be triclinic P-1, and the refined structural parameters are $a = 8.1457(99)$ Å, $b = 9.8032(82)$ Å, $c = 6.6334(72)$ Å, $\alpha = 103.825(3)°$, $\beta = 102.361(0)°$, and $\gamma = 106.992(4)°$. The results are consistent with earlier reports.[29−31] More detailed structural parameters are displayed in Table 1.

Figure 2a shows the magnetic susceptibility χ as a function of temperature measured at various magnetic fields H. Two anomalies are found at $T_{N1} \sim 9.9$ K and $T_{N2} \sim 8.6$ K under

Table 1. Refined Structure Information of $LiCuFe_2(VO_4)_3$ from Powder X-Ray Diffraction at Room T[a]

atom (Wyck.)	x	y	z	occ.	site
Li1	0.0000	0.0000	0.0000	1.000	1a
Li2	0.0909(3)	0.0743(0)	0.5118(5)	0.500	2i
Cu1	0.7780(0)	0.2847(5)	0.2667(9)	1.000	2i
Fe1	0.4493(7)	0.0969(3)	0.3716(1)	1.000	2i
Fe2	0.6990(2)	0.5106(4)	0.0343(0)	1.000	2i
V1	0.6015(6)	0.8320(9)	0.1164(9)	1.000	2i
V2	0.2257(7)	0.3740(1)	0.4082(9)	1.000	2i
V3	0.1565(2)	0.7601(0)	0.2336(9)	1.000	2i
O1	0.0205(0)	0.2524(2)	0.2885(2)	1.000	2i
O2	0.5446(5)	−0.0985(6)	0.3396(7)	1.000	2i
O3	0.2700(4)	0.4442(0)	0.2607(5)	1.000	2i
O4	0.3175(1)	0.2325(2)	0.4085(1)	1.000	2i
O5	0.2700(7)	0.7617(8)	0.4707(5)	1.000	2i
O6	0.5658(9)	0.6527(0)	0.0913(7)	1.000	2i
O7	0.8239(9)	−0.0968(7)	0.1619(6)	1.000	2i
O8	0.5070(1)	0.1539(7)	0.1606(1)	1.000	2i
O9	0.7816(0)	0.3336(8)	−0.0018(1)	1.000	2i
O10	0.7187(0)	0.4874(9)	0.3396(7)	1.000	2i
O11	0.1921(9)	−0.0632(8)	0.2165(8)	1.000	2i
O12	−0.0562(6)	0.6712(0)	0.1997(9)	1.000	2i

[a]Space group: P-1, $a = 8.1457(99)$ Å, $b = 9.8032(82)$ Å, $c = 6.6334(72)$ Å, $\alpha = 103.825(3)°$, $\beta = 102.361(0)°$, $\gamma = 106.992(4)°$, $R_p = 3.04\%$, $R_{wp} = 3.89\%$, and $\chi^2 = 1.121$.

https://doi.org/10.1021/acs.inorgchem.1c02995
Inorg. Chem. 2022, 61, 944−949

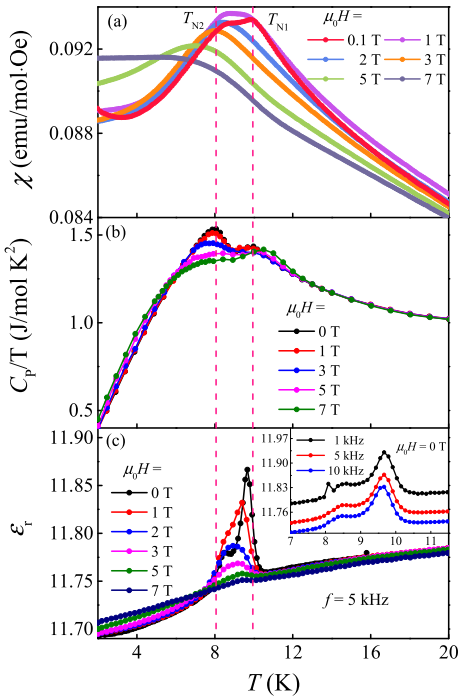

Figure 2. (a) T-dependent magnetic susceptibility under different H. (b) T-dependent C_p/T of $LiCuFe_2(VO_4)_3$ under different H. (c) The dielectric constant ε_r under different H with f = 5 kHz. The inset shows the T dependence of ε_r with various frequencies under zero H.

μ_0H = 0.1 T, indicating the onset of long-range magnetic ordering (LRO). With increasing H, the peaks of $\chi(T)$ slowly drift to lower T and become broader. This suggests that the LRO of $LiCuFe_2(VO_4)_3$ is suppressed by H, which is a typical behavior of a AFM system.[34,35] To further check the magnetic transition of $LiCuFe_2(VO_4)_3$, we measured the specific heat C_p of $LiCuFe_2(VO_4)_3$ under different H. Similarly, the C_p/T of $LiCuFe_2(VO_4)_3$ under zero H exhibits two serial peaks at T_{N1} ∼ 9.95 K and T_{N2} ∼ 8.17 K, as shown in Figure 2b. With increasing H, the peak at T_{N2} drifts to lower T and is suppressed. The specific heat measurement verifies that the AFM transitions of $LiCuFe_2(VO_4)_3$ are suppressed by H, which is consistent with $\chi(T)$ curves.

As to the electrical measurements, the dielectric constants $\varepsilon_r(T)$ is measured first, as presented in Figure 2c. The $\varepsilon_r(T)$ exhibits a sharp peak at T_{N1} and a step-like anomaly at T_{N2} under zero H, as shown in the inset of Figure 2c. These two anomalies do not shift with increasing measuring frequency, ruling out the possibility of artifactual signals from defects' relaxation. Then, the magneto-dielectric effect is investigated. As shown in Figure 2c, the two anomalies are significantly suppressed and drift to lower T with increasing H. Also, the anomalies are almost unrecognizable at μ_0H = 7 T. These results are consistent with $\chi(T)$ and C_p data. The remarkable magneto-dielectric effect hints the existence of ferroelectricity and a remarkable ME effect. Actually, previous studies have claimed the multiferroicity of $LiCuFe_2(VO_4)_3$ by discussing the dielectric signals,[30,31] but the direct ferroelectric measurements are still missing.

The pyroelectric current $I_{pyro}(T)$ is measured to reveal the electrical polarization of $LiCuFe_2(VO_4)_3$. Figure 3a shows $I_{pyro}(T)$ of $LiCuFe_2(VO_4)_3$ obtained at various heating rates (2, 4, and 6 K/min) under poling electric field E_p = 3.33 kV/cm and zero magnetic field. Interestingly, two current peaks with

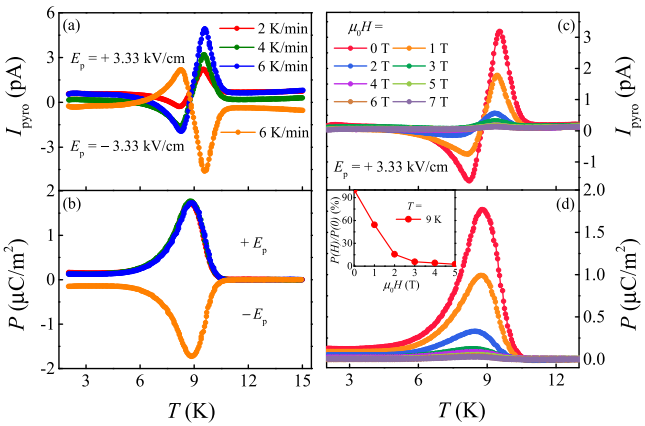

Figure 3. (a) Pyroelectric current of $LiCuFe_2(VO_4)_3$ measured at various heating rates: 2, 4, and 6 K/min under E_p = ±3.33 kV/cm and μ_0H = 0 T. (b) T-dependent ferroelectric polarization derived by integrating the pyroelectric current relative to time under E_p = ±3.33 kV/cm and μ_0H = 0 T. (c) Pyroelectric current and (d) corresponding ferroelectric polarization of $LiCuFe_2(VO_4)_3$ under various H and E_p = ±3.33 kV/cm. Inset: the ME effect at T = 9 K.

opposite directions are observed at T_{N1} and T_{N2}, respectively. The current peaks are un-shifted with various heating rates, indicating that the current signals are indeed from pyroelectric effect. Besides, the poling with a negative electric field indeed leads to a reversal of $I_{pyro}(T)$, as demonstrated in Figure 3a. Figure 3b presents the $P(T)$ curves obtained by integrating the $I_{pyro}(T)$. The $P(T)$ curves measured under $\pm E_p$ have similar magnitude with opposite directions, implying that the P can be reversed and thus $LiCuFe_2(VO_4)_3$ is indeed a ferroelectric material. In short, through the combination of $\chi(T)$, C_p, ε_r, and $I_{pyro}(T)$ measurements, we exhibit the simultaneous existence of FE transition and AFM transitions and confirm that $LiCuFe_2(VO_4)_3$ is a magnetically induced multiferroics (i.e., a type-II multiferroic one).

Then, the ME effect of $LiCuFe_2(VO_4)_3$ can be demonstrated by measuring the $I_{pyro}(T)$ curves under different H, and the results are presented in Figure 3c. With increasing H, the two pyroelectric current peaks slightly shift to lower T and the magnitudes decrease simultaneously. It is noted that the pyroelectric current is too weak to be recognized when H is higher than 3 T. Figure 3d depicts the P under different H, which is significantly suppressed with increasing H. Such a behavior is widely observed in many type-II multiferroics, which further suggests that $LiCuFe_2(VO_4)_3$ is one of the cases.[13,36]

DISCUSSION

According to above measurements, it is obvious that $LiCuFe_2(VO_4)_3$ belongs to the type-II multiferroics. On one hand, complicated magnetic interactions were argued to exist between Fe−Cu and Fe−Fe spins in $LiCuFe_2(VO_4)_3$,[29,30] which might lead to frustrated spin states like non-collinear spin texture with the incommensurate/commensurate period. On the other hand, the P of $LiCuFe_2(VO_4)_3$ is highly susceptible to H, which can be attributed to the change in spin texture under H. Both these characteristics are features of type-II multiferroics. Besides these common characteristics, the multiferroicity in $LiCuFe_2(VO_4)_3$ is special for its two pyroelectric current peaks. There are two possibilities to explain this nontrivial behavior.

https://doi.org/10.1021/acs.inorgchem.1c02995
Inorg. Chem. 2022, 61, 944−949

The first possibility is that these two peaks could be from two independent ferroelectric components with different transition points, like recently proposed "irreducible ferrielectricity".[37] In $LiCuFe_2(VO_4)_3$, there are two different magnetic ions (Cu^{2+} and Fe^{3+}), and Fe^{3+} ions have two nonequivalent positions. Therefore, these Cu^{2+} and Fe^{3+} ions may order at different temperatures and form two different sublattices which contribute to the net P independently. Similar scenarios can be referred to extensively researched RMn_2O_5[38−40] and $DyMnO_3$.[41,42] In RMn_2O_5, two ferroelectric components are identified, which originate from Mn^{3+}-Mn^{4+}-Mn^{3+} blocks and R^{3+}-Mn^{4+}-R^{3+} blocks, respectively.[43,44] In $DyMnO_3$, the Mn sublattice and Dy sublattice order at different temperatures and contribute to the net polarization in opposite directions.[41,42]

The second possibility is that the two current peaks correspond to sequential magnetic transitions. Before T_{N1}, the paramagnetic (PM) phase is nonpolar, and the AFM phase below T_{N2} is also nonpolar. Only the AFM phase between T_{N1} and T_{N2} breaks the spatial inversion symmetry and generates the polarization. Such scenarios of intermediate multiferroic phases have also been found in $MnWO_4$, $Ni_3V_2O_8$, and CuO.[27,45−50] In these materials, multiple magnetic transitions take place at different temperatures and the ferroelectricity only exists in the temperature windows of incommensurate magnetic structures.[27,45−48]

According to above discussions, the complicated magnetic interaction in $LiCuFe_2(VO_4)_3$ allows the presence of two sequential magnetic transitions. Thus, the second scenario seems to be much more likely than the first one. To further verify this scenario, the sample was cooled down to 2 K without poling electric field and then poled from 2 to 9 K under an electric field E = ±3.33 kV/cm. Then, the pyroelectric current of $LiCuFe_2(VO_4)_3$ was measured during the heating or cooling of the samples. As shown in Figure 4a,

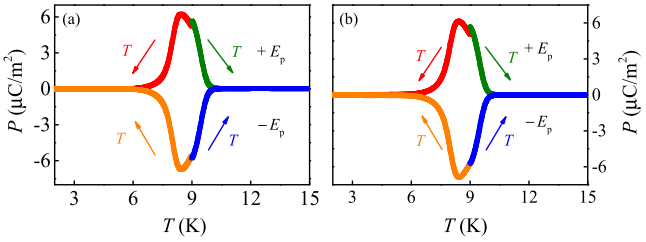

Figure 4. Ferroelectric polarization of $LiCuFe_2(VO_4)_3$. The corresponding pyroelectric current was measured when cooling the sample from 9 to 2 K (red and orange) or heating the sample from 9 to 15 K (green and blue). (a) With a poling process from 2 to 9 K. (b) With a poling process from 20 to 9 K. The poling field is fixed as E_p = ±3.33 kV/cm.

the ferroelectric polarization P only exists between T_{N2} and T_{N1}, while it is negligible in other regions. Besides, this P is identical to the case with poling from 20 to 9 K, as compared in Figure 4b. Hence, we are confident that $LiCuFe_2(VO_4)_3$ is similar to CuO, which belongs to the family of intermediate multiferroic systems. Of course, the magnetic structure of $LiCuFe_2(VO_4)_3$ has not been resolved yet. In future, neutron diffraction experiments are desired to clarify this issue by solving the magnetic structures of $LiCuFe_2(VO_4)_3$ between T_{N1} and T_{N2} and below T_{N2}.

Based on the second scenario, the magnetic and polar phase diagram for $LiCuFe_2(VO_4)_3$ is plotted in Figure 5, according to

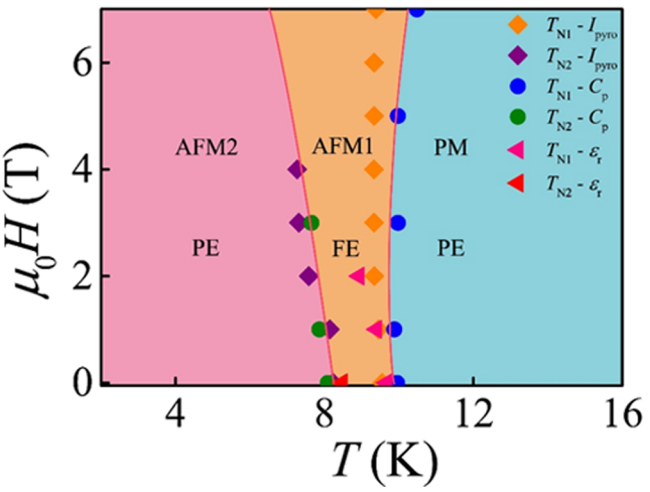

Figure 5. Magnetic and polar phase diagram for $LiCuFe_2(VO_4)_3$ determined by aforementioned measurements. The multiferroic phase exists only in the intermediate window.

above measurements. It is PM and paraelectric (PE) above T_{N1} ~ 9.95 K. When the T decreases to T_{N1}, $LiCuFe_2(VO_4)_3$ undergoes the first AFM phase transition (so called AFM1 phase), and simultaneously, a ferroelectric phase transition (FE phase) occurs at T_{N1}. As T further decreases, another AFM transition (so called AFM2 phase) occurs at T_{N2} ~ 8.17 K. The AFM2 phase transition leads to the disappearance of ferroelectricity. Therefore, $LiCuFe_2(VO_4)_3$ is marked as PE below T_{N2}. The applied magnetic field can slightly expand this multiferroic window. Under the magnetic field, the anomaly signal can slightly broad the ferroelectric phase region, which may be related to the possible frustrated spin structure. Maybe the magnetic field can suppress the frustration, which enhances the ordering temperature slightly.

CONCLUSIONS

In summary, we have systematically investigated the magnetism and multiferroicity in mixed spin-chain $LiCuFe_2(VO_4)_3$. Magnetic susceptibility and specific heat showed two adjacent AFM transitions at T_{N1} ~ 9.95 K and T_{N2} ~ 8.17 K. Pyroelectric current and dielectric measurements confirmed the FE transition at T_{N1}. Interestingly, two sign-opposite pyroelectric peaks are observed at T_{N1} and T_{N2}, giving rise to a reentrant PE phase below T_{N2}. Moreover, the FE P of $LiCuFe_2(VO_4)_3$ is very sensitive to magnetic fields, that is, it exhibits a significant ME effect. We suggest that the sequential magnetic transitions lead to this special multiferroic behavior, namely, only the intermediate AFM1 phase can induce polarization. Furthermore, studies using single-crystal samples and neutron experiments are encouraged to verify our proposal of multiferroicity in $LiCuFe_2(VO_4)_3$.

AUTHOR INFORMATION

Corresponding Authors

Meifeng Liu − *Institute for Advanced Materials, Hubei Normal University, Huangshi 435002, China;* orcid.org/0000-0001-5733-8764; Email: lmfeng1107@hbnu.edu.cn

Shuai Dong − *School of Physics, Southeast University, Nanjing 211189, China;* orcid.org/0000-0002-6910-6319; Email: sdong@seu.edu.cn

https://doi.org/10.1021/acs.inorgchem.1c02995
Inorg. Chem. 2022, 61, 944−949

Authors

Xiyu Chen − *Institute for Advanced Materials, Hubei Normal University, Huangshi 435002, China*

Shuhan Zheng − *Institute for Advanced Materials, Hubei Normal University, Huangshi 435002, China*

Tao Zou − *Collaborative Innovation Center of Light Manipulations and Applications, Shangdong Normal University, Jinan 250358, China*

Wei Wang − *Institute for Advanced Materials, South China Academy of Advanced Optoelectronics, South China Normal University, Guangzhou 510006, China*

Keer Nie − *Institute for Advanced Materials, Hubei Normal University, Huangshi 435002, China*

Fei Liu − *Institute for Advanced Materials, Hubei Normal University, Huangshi 435002, China*

Yunlong Xie − *Institute for Advanced Materials, Hubei Normal University, Huangshi 435002, China*

Min Zeng − *Institute for Advanced Materials, South China Academy of Advanced Optoelectronics, South China Normal University, Guangzhou 510006, China;* orcid.org/0000-0003-3594-7619

Xiuzhang Wang − *Institute for Advanced Materials, Hubei Normal University, Huangshi 435002, China*

Hong Li − *Institute for Advanced Materials, Hubei Normal University, Huangshi 435002, China*

Jun-Ming Liu − *Institute for Advanced Materials, Hubei Normal University, Huangshi 435002, China; Laboratory of Solid State Microstructures, Nanjing University, Nanjing 210093, China;* orcid.org/0000-0001-8988-8429

Complete contact information is available at: https://pubs.acs.org/10.1021/acs.inorgchem.1c02995

Author Contributions

#X.C. and S.Z. contribute equally to this work.

Notes

The authors declare no competing financial interest.

■ ACKNOWLEDGMENTS

This work was supported by the National Natural Science Foundation of China (grant nos. 11834002, 12074111, 92163210, and 11704109). The Research Project of Hubei Provincial Department of Education (grant no. Q20202502).

■ REFERENCES

(1) Dong, S.; Liu, J.-M.; Cheong, S.-W.; Ren, Z. Multiferroic materials and magnetoelectric physics: symmetry, entanglement, excitation, and topology. *Adv. Phys.* **2015**, *64*, 519−626.

(2) Fiebig, M.; Lottermoser, T.; Meier, D.; Trassin, M. The evolution of multiferroics. *Nat. Rev. Mater.* **2016**, *1*, 16046.

(3) Dong, S.; Xiang, H.; Dagotto, E. Magnetoelectricity in multiferroics: a theoretical perspective. *Natl. Sci. Rev.* **2019**, *6*, 629−641.

(4) Spaldin, N. A.; Ramesh, R. Advances in magnetoelectric multiferroics. *Nat. Mater.* **2019**, *18*, 203−212.

(5) Lu, C.; Wu, M.; Lin, L.; Liu, J.-M. Single-phase multiferroics: new materials, phenomena, and physics. *Natl. Sci. Rev.* **2019**, *6*, 653−668.

(6) Schoenherr, P.; Manz, S.; Kuerten, L.; Shapovalov, K.; Iyama, A.; Kimura, T.; Fiebig, M.; Meier, D. Local electric-field control of multiferroic spin-spiral domains in $TbMnO_3$. *npj Quantum Mater.* **2020**, *5*, 86.

(7) Kimura, K.; Kato, Y.; Kimura, S.; Motome, Y.; Kimura, T. Crystal-chirality-dependent control of magnetic domains in a time-reversal-broken antiferromagnet. *npj Quantum Mater.* **2021**, *6*, 54.

(8) Cheong, S.-W.; Mostovoy, M. Multiferroics: a magnetic twist for ferroelectricity. *Nat. Mater.* **2007**, *6*, 13−20.

(9) Khomskii, D. Classifying multiferroics: Mechanisms and effects. *Physics* **2009**, *2*, 20.

(10) Sergienko, I. A.; Dagotto, E. Role of the Dzyaloshinskii-Moriya interaction in multiferroic perovskites. *Phys. Rev. B: Condens. Matter Mater. Phys.* **2006**, *73*, 094434.

(11) Murakawa, H.; Onose, Y.; Miyahara, S.; Furukawa, N.; Tokura, Y. Ferroelectricity Induced by Spin-Dependent Metal-Ligand Hybridization in $Ba_2CoGe_2O_7$. *Phys. Rev. Lett.* **2010**, *105*, 137202.

(12) Murakawa, H.; Onose, Y.; Miyahara, S.; Furukawa, N.; Tokura, Y. Comprehensive study of the ferroelectricity induced by the spin-dependentd-phybridization mechanism in $Ba_2XGe_2O_7$(X= Mn, Co, and Cu). *Phys. Rev. B: Condens. Matter Mater. Phys.* **2012**, *85*, 174106.

(13) Choi, Y. J.; Yi, H. T.; Lee, S.; Huang, Q.; Kiryukhin, V.; Cheong, S. W. Ferroelectricity in an Ising Chain Magnet. *Phys. Rev. Lett.* **2008**, *100*, 047601.

(14) Wu, H.; Burnus, T.; Hu, Z.; Martin, C.; Maignan, A.; Cezar, J. C.; Tanaka, A.; Brookes, N. B.; Khomskii, D. I.; Tjeng, L. H. Ising Magnetism and Ferroelectricity in Ca_3CoMnO_6. *Phys. Rev. Lett.* **2009**, *102*, 026404.

(15) Zhang, G.; Dong, S.; Yan, Z.; Guo, Y.; Zhang, Q.; Yunoki, S.; Dagotto, E.; Liu, J.-M. Multiferroic properties of $CaMn_7O_{12}$. *Phys. Rev. B: Condens. Matter Mater. Phys.* **2011**, *84*, 174413.

(16) Zhou, L.; Dai, J.; Chai, Y.; Zhang, H.; Dong, S.; Cao, H.; Calder, S.; Yin, Y.; Wang, X.; Shen, X.; Liu, Z.; Saito, T.; Shimakawa, Y.; Hojo, H.; Ikuhara, Y.; Azuma, M.; Hu, Z.; Sun, Y.; Jin, C.; Long, Y. Realization of Large Electric Polarization and Strong Magnetoelectric Coupling in $BiMn_3Cr_4O_{12}$. *Adv. Mater.* **2017**, *29*, 1703435.

(17) Wang, X.; Chai, Y.; Zhou, L.; Cao, H.; Cruz, C. D.; Yang, J.; Dai, J.; Yin, Y.; Yuan, Z.; Zhang, S.; Yu, R.; Azuma, M.; Shimakawa, Y.; Zhang, H.; Dong, S.; Sun, Y.; Jin, C.; Long, Y. Observation of Magnetoelectric Multiferroicity in a Cubic Perovskite System: $LaMn_3Cr_4O_{12}$. *Phys. Rev. Lett.* **2015**, *115*, 087601.

(18) Liu, M.; Lin, L.; Zhang, Y.; Li, S.; Huang, Q.; Garlea, V. O.; Zou, T.; Xie, Y.; Wang, Y.; Lu, C.; Yang, L.; Yan, Z.; Wang, X.; Dong, S.; Liu, J.-M. Cycloidal magnetism driven ferroelectricity in double tungstate $LiFe(WO_4)_2$. *Phys. Rev. B* **2017**, *95*, 195134.

(19) Wang, Z.; Lorenz, T.; Gorbunov, D. I.; Cong, P. T.; Kohama, Y.; Niesen, S.; Breunig, O.; Engelmayer, J.; Herman, A.; Wu, J.; Kindo, K.; Wosnitza, J.; Zherlitsyn, S.; Loidl, A. Quantum Criticality of an Ising-like Spin-1/2 Antiferromagnetic Chain in a Transverse Magnetic Field. *Phys. Rev. Lett.* **2018**, *120*, 207205.

(20) Cui, Y.; Zou, H.; Xi, N.; He, Z.; Yang, Y. X.; Shu, L.; Zhang, G. H.; Hu, Z.; Chen, T.; Yu, R.; Wu, J.; Yu, W. Quantum Criticality of the Ising-like Screw Chain Antiferromagnet $SrCo_2V_2O_8$ in a Transverse Magnetic Field. *Phys. Rev. Lett.* **2019**, *123*, 067203.

(21) Bera, A. K.; Lake, B.; Islam, A. T. M. N.; Klemke, B.; Faulhaber, E.; Law, J. M. Field-induced magnetic ordering and single-ion anisotropy in the quasi-one-dimensional Haldane chain compound $SrNi_2V_2O_8$: A single-crystal investigation. *Phys. Rev. B: Condens. Matter Mater. Phys.* **2013**, *87*, 224423.

(22) Dutton, S. E.; Kumar, M.; Mourigal, M.; Soos, Z. G.; Wen, J.-J.; Broholm, C. L.; Andersen, N. H.; Huang, Q.; Zbiri, M.; Toft-Petersen, R.; Cava, R. J. Quantum Spin Liquid in Frustrated One-Dimensional $LiCuSbO_4$. *Phys. Rev. Lett.* **2012**, *108*, 187206.

(23) Park, S.; Choi, Y. J.; Zhang, C. L.; Cheong, S. W. Ferroelectricity in an S =1/2 Chain Cuprate. *Phys. Rev. Lett.* **2007**, *98*, 057601.

(24) Schrettle, F.; Krohns, S.; Lunkenheimer, P.; Hemberger, J.; Büttgen, N.; Krug von Nidda, H.-A.; Prokofiev, A. V.; Loidl, A. Switching the ferroelectric polarization in the S =1/2 chain cuprate $LiCuVO_4$ by external magnetic fields. *Phys. Rev. B: Condens. Matter Mater. Phys.* **2008**, *77*, 144101.

(25) Ding, L.; Manuel, P.; Khalyavin, D. D.; Orlandi, F.; Tsirlin, A. A. Unraveling the complex magnetic structure of multiferroic pyroxene $NaFeGe_2O_6$: A combined experimental and theoretical study. *Phys. Rev. B* **2018**, *98*, 094416.

(26) Colin, C. V.; Ding, L.; Ressouche, E.; Robert, J.; Terada, N.; Gay, F.; Lejay, P.; Simonet, V.; Darie, C.; Bordet, P.; Petit, S. Incommensurate spin ordering and excitations in multiferroic $SrMnGe_2O_6$. *Phys. Rev. B* **2020**, *101*, 235109.
(27) Taniguchi, K.; Abe, N.; Takenobu, T.; Iwasa, Y.; Arima, T. Ferroelectric Polarization Flop in a Frustrated Magnet $MnWO_4$ Induced by a Magnetic Field. *Phys. Rev. Lett.* **2006**, *97*, 097203.
(28) Belik, A. A. Synthesis and crystal structure of LiCuFe2(VO4)3 by rietveld method. *Mater. Res. Bull.* **1999**, *34*, 1973−1980.
(29) Drokina, T. V.; Petrakovskii, G. A.; Bayukov, O. A.; Vorotynov, A. M.; Velikanov, D. A.; Molokeev, M. S. Synthesis and Structural, Magnetic, and Resonance Properties of the $LiCuFe_2(VO_4)_3$ Compound. *Phys. Solid State* **2016**, *58*, 1981−1988.
(30) Koshelev, A. V.; Zakharov, K. V.; Pyatakov, A. P.; Shvanskaya, L. V.; Shakin, A. A.; Volkova, O. S.; Chareev, D. A.; Kamusella, S.; Klauss, H.-H.; Molla, K.; Rahaman, B.; Saha-Dasgupta, T.; Vasiliev, A. N. Spin-Order-Induced Ferroelectricity and Magnetoelectric Effect in $LiCuFe_2(VO_4)_3$. *Phys. Rev. Appl.* **2018**, *10*, 034008.
(31) Koshelev, A.; Shvanskaya, L.; Volkova, O.; Zakharov, K.; Theuss, F.; Koo, C.; Klingeler, R.; Kamusella, S.; Klauss, H.-H.; Kundu, S.; Bachhar, S.; Mahajan, A. V.; Khuntia, P.; Khanam, D.; Rahaman, B.; Saha-Dasgupta, T.; Vasiliev, A. Thermodynamic and resonant properties of mixed spin compounds $ACuFe_2(VO_4)_3$ (A = Li, Na). *J. Alloys Compd.* **2020**, *842*, 155763.
(32) Toby, B. H. EXPGUI, a graphical user interface for GSAS. *J. Appl. Crystallogr.* **2001**, *34*, 210.
(33) Toby, B. H.; Von Dreele, R. B. GSAS-II: the genesis of a modern open-source all purpose crystallography software package. *J. Appl. Crystallogr.* **2013**, *46*, 544−549.
(34) He, Z.; Taniyama, T.; Kyômen, T.; Itoh, M. Field-induced order-disorder transition in the quasi-one-dimensional anisotropic antiferromagnet $BaCo_2V_2O_8$. *Phys. Rev. B: Condens. Matter Mater. Phys.* **2005**, *72*, 172403.
(35) Liu, M.; Zhang, H.; Huang, X.; Ma, C.; Dong, S.; Liu, J.-M. Two-Step Antiferromagnetic Transitions and Ferroelectricity in Spin-1 Triangular-Lattice Antiferromagnetic $Sr_3NiTa_2O_9$. *Inorg. Chem.* **2016**, *55*, 2709−2716.
(36) Hwang, J.; Choi, E. S.; Ye, F.; Dela Cruz, C. R.; Xin, Y.; Zhou, H. D.; Schlottmann, P. Successive Magnetic Phase Transitions and Multiferroicity in the Spin-One Triangular-Lattice Antiferromagnet $Ba_3NiNb_2O_9$. *Phys. Rev. Lett.* **2012**, *109*, 257205.
(37) Du, K.; Guo, L.; Peng, J.; Chen, X.; Zhou, Z.-N.; Zhang, Y.; Zheng, T.; Liang, Y.-P.; Lu, J.-P.; Ni, Z.-H.; Wang, S.-S.; Van Tendeloo, G.; Zhang, Z.; Dong, S.; Tian, H. Direct visualization of irreducible ferrielectricity in crystals. *npj Quantum Mater.* **2020**, *5*, 49.
(38) Higashiyama, D.; Miyasaka, S.; Tokura, Y. Magnetic-field-induced polarization and depolarization in $HoMn_2O_5$ and $ErMn_2O_5$. *Phys. Rev. B: Condens. Matter Mater. Phys.* **2005**, *72*, 064421.
(39) Hur, N.; Park, S.; Sharma, P. A.; Ahn, J. S.; Guha, S.; Cheong, S.-W. Electric polarization reversal and memory in a multiferroic material induced by magnetic fields. *Nature* **2004**, *429*, 392−395.
(40) Higashiyama, D.; Miyasaka, S.; Kida, N.; Arima, T.; Tokura, Y. Control of the ferroelectric properties of $DyMn_2O_5$ by magnetic fields. *Phys. Rev. B: Condens. Matter Mater. Phys.* **2004**, *70*, 174405.
(41) Zhang, N.; Guo, Y. Y.; Lin, L.; Dong, S.; Yan, Z. B.; Li, X. G.; Liu, J.-M. Ho substitution suppresses collinear Dy spin order and enhances polarization in $DyMnO_3$. *Appl. Phys. Lett.* **2011**, *99*, 102509.
(42) Zhang, N.; Dong, S.; Zhang, G. Q.; Lin, L.; Guo, Y. Y.; Liu, J.-M.; Ren, Z. F. Multiferroic phase diagram of Y partially substituted $Dy_{1-x}Y_xMnO_3$. *Appl. Phys. Lett.* **2011**, *98*, 012510.
(43) Zhao, Z. Y.; Liu, M. F.; Li, X.; Lin, L.; Yan, Z. B.; Dong, S.; Liu, J.-M. Experimental observation of ferrielectricity in multiferroic $DyMn_2O_5$. *Sci. Rep.* **2014**, *4*, 3984.
(44) Liu, J.-M.; Dong, S. Ferrielectricity in $DyMn_2O_5$: A golden touchstone for multiferroicity of RMn_2O_5 family. *J. Adv. Dielectr.* **2015**, *05*, 1530003.
(45) Arkenbout, A. H.; Palstra, T. T. M.; Siegrist, T.; Kimura, T. Ferroelectricity in the cycloidal spiral magnetic phase of $MnWO_4$. *Phys. Rev. B: Condens. Matter Mater. Phys.* **2006**, *74*, 184431.
(46) Lawes, G.; Harris, A. B.; Kimura, T.; Rogado, N.; Cava, R. J.; Aharony, A.; Entin-Wohlman, O.; Yildirim, T.; Kenzelmann, M.; Broholm, C.; Ramirez, A. P. Magnetically Driven Ferroelectric Order in $Ni_3V_2O_8$. *Phys. Rev. Lett.* **2005**, *95*, 087205.
(47) Kimura, T.; Sekio, Y.; Nakamura, H.; Siegrist, T.; Ramirez, A. P. Cupric oxide as an induced-multiferroic with high-T_C. *Nat. Mater.* **2008**, *7*, 291−294.
(48) Wang, Z.; Qureshi, N.; Yasin, S.; Mukhin, A.; Ressouche, E.; Zherlitsyn, S.; Skourski, Y.; Geshev, J.; Ivanov, V.; Gospodinov, M.; Skumryev, V. Magnetoelectric effect and phase transitions in CuO in external magnetic fields. *Nat. Commun.* **2016**, *7*, 10295.
(49) Taniguchi, K.; Abe, N.; Ohtani, S.; Arima, T. Magnetoelectric memory effect of the nonpolar phase with collinear spin structure in multiferroic $MnWO_4$. *Phys. Rev. Lett.* **2009**, *102*, 147201.
(50) Wu, W. B.; Huang, D. J.; Okamoto, J.; Huang, S. W.; Sekio, Y.; Kimura, T.; Chen, C. T. Multiferroic nanoregions and a memory effect in cupric oxide. *Phys. Rev. B: Condens. Matter Mater. Phys.* **2010**, *81*, 172409.

https://doi.org/10.1021/acs.inorgchem.1c02995
Inorg. Chem. 2022, 61, 944−949